

## **THE COMPARISON OF COHESIVE SOIL DAMPING RATIOS OBTAINED FROM RESONANT COLUMN TESTS AND DESIGNATED BY THE FREE-VIBRATION DECAY AND HALF-POWER BANDWIDTH METHOD**

Wojciech Sas

Warsaw University of Life Sciences – SGGW

**Abstract.** One of the aims of modern laboratory studies is searching for dynamic parameters in a small strain of a soil. The reason behind this trend is the higher level of density of urban areas. City traffic, including trams, cars and subway trains, as well as certain types of construction works, can generate seismic waves, which cause a small strain between the soil and the structure to occur. This may lead to an exceeded limit serviceability state. The three main dynamic parameters of the soil are: Young modulus, shear modulus and damping ratio. Estimation of the cohesive soils damping ratio by two methods, namely free-vibration decay and half-power bandwidth, is the main goal of this article. The author performed his own research on two silty clay specimens in a resonant column. The conducted research show that the damping ratio obtained by using the half-power bandwidth method has significant error margin, which is equal approximately 50–60%, yet the curve shapes are very similar to the ones obtained by using the second method discussed in this paper. In author's opinion, more research on cohesive soils has to be performed in order to introduce necessary corrections to half-power bandwidth equations.

**Key words:** free-vibration decay, half-power bandwidth, damping ratio, resonant column

### **INTRODUCTION**

In recent times, dynamic soil parameters are usually determined both from laboratory and field tests, but it is difficult to obtain a strain-dependent curve of the shear modulus ( $G$ ) and the damping ratio ( $D$ ) directly from in-situ tests [Ishihara 1996]. Every laboratory testing technique distinguishes between the boundary condition, the working strain amplitude and frequency. Dynamic analysis tests such as the resonant column (RC), cyclic

---

Corresponding author: Wojciech Sas, Warsaw University of Life Sciences, Faculty of Civil and Environmental Engineering, Water Center Laboratory, St. Ciszewskiego 6, 02-776 Warsaw, e-mail: wojciech\_sas@sggw.pl

© Copyright by Wydawnictwo SGGW, Warszawa 2016

triaxial (CTX), cyclic simple shear (CSS) or cyclic torsional shear (TS) test, can provide  $G$  and  $D$  curves. The results obtained from those tests are widely accepted by the engineers and designers. A different method, based on the measurement of the seismic wave velocities, makes use of the piezoelectric transducers, e.g. bender elements (BE) [Gabryś et al. 2015]. The research methods mentioned above are described in [Ishihara 1996, Das and Ramana 2010].

One of the most reliable values of the dynamic soil parameter can be obtained, by using the resonant column apparatus. The biggest advantage of this device is the working range of strain, which spans from small ( $1 \cdot 10^{-5}\%$ ) to medium ( $1 \cdot 10^{-2}\%$ ) strain [Gabryś et al. 2015]. The above-mentioned range of deformations is very important for designers of underground structures. Moreover, the dynamic properties are used more frequently in designing roads and railway lines [Lim et al. 2013]. The anisotropic consolidation possibility [Sun et al. 2013] was introduced in RC in order to better reflect the in-situ conditions. A new research technique [Camacho Tauta et al. 2010] was also implemented in order to obtain more reliable results from the RC tests.

This article focuses on the dynamic soil parameter  $D$ , because of its high difficulty in interpretation and problematic methodology for its determination in cohesive soils. The paper contains a review of literature concerning  $D$  obtained by the free-vibration decay (FVD) and half-power bandwidth method (HPB), a description of the methodology used in the research and a specification of the resonant column used in the experiment. The results of the author's own RC tests and  $D$ , determined by using both methods, can also be found in the publication, as well as the conclusions drawn from the research.

## LITERATURE REVIEW

The  $D$  is commonly used in structural design. The most popular method for determining the value of  $D$  is the collocation method and two energetic methods, namely potential, kinetic and HPB procedure. In Flaga et al. [2008], the authors describe each of the abovementioned approaches and verify them. The scientists have created two real compound- and two numerical models. Damping results obtained using the numerical method were in better agreement than the outcome of the model investigation, but in both cases differences between the acquired  $D$  increase, along with the increase in vibration frequency [Flaga et al. 2008].

One of the new trends in designing is to consider the importance of soil damping in seismic responses of soil-structures system. This phenomenon was studied by Ahmadi et al. in [2015]. In order to examine this problem, a superstructure was modelled as a two-dimensional nonlinear multi-story shear building. Soil under the foundation was assumed to be based on the concept of the cone model. The relative reduction ratios were used for the investigation of the effect of various parameters. The tests prove that soil damping should be included in the seismic analysis of soil-structure, when the superstructure becomes slender [Ahmadi et al. 2015].

Because of many numerical research attempts at proving the validity of the  $D$  in soil-structures system, numerous scientists examine the dynamic properties of soils in their laboratories. The most reliable laboratory technique of obtaining the dynamic parameters is

the one using the RC tests, because the maximum shear modulus  $G_{\min}$  and the minimum damping ratio  $D_{\min}$  can be determined at a very low strain level (approximately  $\approx 10^{-5}\%$ ), generated by said apparatus. In order to establish the relationship between the normalized shear modulus ( $G/G_{\max}$ ) and  $D$ , the authors of Zhang et al. [2005] took into consideration 122 results of RC and TS tests on the Quaternary, Tertiary and the residual/saprolite soil specimens from South Carolina, North Carolina and Alabama. They created equations allowing to calculate the  $D$ , which are expressed by a polynomial function of the normalized shear modulus ( $G/G_{\max}$ ) plus a  $D_{\min}$ . It turned out that the Quaternary soils exhibit more linearity than other soils. The Researchers have also examined the influence of the plasticity index on the dynamic characteristics of soils and found out that plasticity index has lesser impact on dynamic soil behaviour than thought previously Zhang et al. [2005].

The new methodology of determining  $D$  using the free-decay response can be found in Tallavo et al. [2013]. The authors presented a new analysis, based on the complex exponential method for nonlinear dynamic characterization of soil specimens in torsional fixed-free RC testing. Less popular steady-state method for determining  $D$  is described and compared to the FVD method in Senetakis et al. [2015]. It has been established that the results of both approaches in most display differences lying in the acceptable range of 15%. The process of obtaining the  $D$  value by using HPB and FVD methods is presented by Hoyos et al. [2013]. Said paper is focused on the unsaturated properties of silty sand, thus meaning that the  $D$  is dependent on the matric suction.

In order to check the utility of the classic approach, based on using the HPB method to estimate the  $D$  value for cohesive soils, the following comparison was conducted. Based on many conducted researches and much results interpretation experience the author selected FVD as a reference method. Although author did not suggests that FVD method is the only proper and correct technique for measure  $D$ .

## MATERIALS AND METHODS

### Free – vibration decay method

The  $D$  in standard RC damping test is calculated on the basis of the free-vibration curve shape. This curve is measured by the accelerometer installed on the resonant column drive plate. A torsional motion is applied to the sample for the time set by user. Next, the excitation is shut off and the free vibrations decay is measured by the accelerometer (Fig. 1).

The logarithmic decrement ( $\delta$ ) is calculated by taking logarithm of the wave amplitudes ratio for successive cycles up until the vibrations are completely extinguished [Hoyos et al. 2013]:

$$\delta = \frac{1}{n} \ln \frac{A_1}{A_{n+1}} \quad (1)$$

where  $n$  stands for the number of cycles until the decay of sample motions from amplitude  $A_1$  to  $A_{n+1}$ .

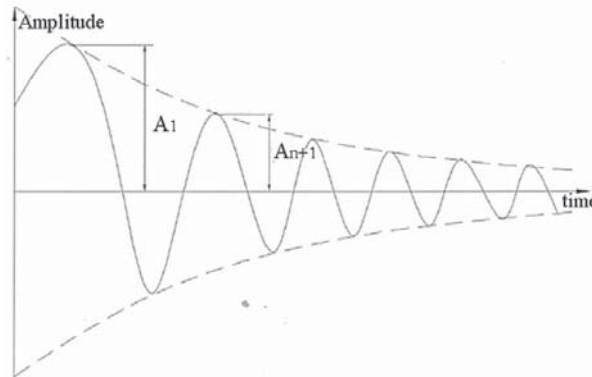


Fig. 1. Free vibration decay curve

The  $D$  is calculated on the basis:

$$D = \sqrt{\frac{\delta^2}{4\pi^2 + \delta^2}} \quad (2)$$

A detailed description of the methodology used for the  $D$  determination and the author's research concerning the impact of the sample oscillation time and cycle number was included in the calculation of the  $D$  can be found in Soból et al. [2015] and Sas et al. [2015a, b].

### Half – power bandwidth method

For the purposes of this article, the author has also used a well-known half-power bandwidth method, based on measuring the resonant frequency of the sample. This method is applicable only in case of a slightly damped single-degree-of-freedom system, but after certain corrections are applied, it can be used in a multi-degree-of-freedom structures, as presented in the literature review.

Due to the sample in resonant column having one degree of freedom, the author adopts a standard half-power bandwidth method. It is then assumed, that half of the total power dissipation occurs in the frequency band between  $f_1$  and  $f_2$ , where  $f_1$  and  $f_2$  are frequencies corresponding to the amplitude of resonant frequency  $f_{res}/\sqrt{2}$  (Fig. 2).

It is shown in Chopra [1995] that the small damping ratio  $\zeta$ , is approximately equal:

$$\zeta = \frac{f_2 - f_1}{2f_{res}} \quad (3)$$

However, if the value of  $\zeta$  is not assumed to be small, the relationship becomes equal:

$$\zeta = \sqrt{0.5 - \sqrt{0.25 - 0.0625 \left( \frac{f_2 - f_1}{f_{res}} \right)^2 \left( \frac{f_2 + f_1}{f_{res}} \right)^2}} \quad (4)$$

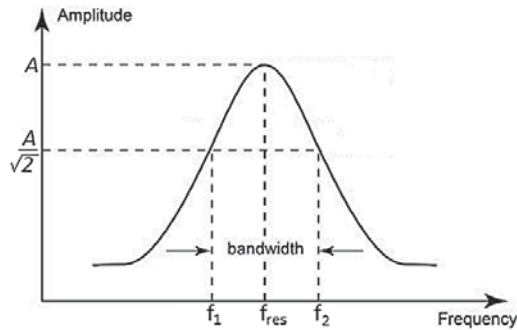


Fig. 2. Definition of the half-power bandwidth

Alternatively, if excitation comes from the mass rotating at an angular velocity of  $\bar{\omega}$  rad/s and since half-power bandwidth presumes a sinusoidal exciting force with a constant amplitude, the modified half-power formula can be used [Butterworth et al. 2004]:

$$\zeta = \frac{f_{res}(f_2 - f_1)}{f_1^2 + f_2^2} \tag{5}$$

The above-mentioned modification was obtained by a numerical simulation of a viscously-damped single-degree-of-freedom system's response to excitation mass. The author then worked backwards to re-calculate the  $\zeta$  [Butterworth et al. 2004].

**Materials**

In order to compare the damping ratios obtained from two different techniques, two samples of the cohesive soil was examined. The first one of the specimen came from the S2 expressway from region of the Warsaw, node Konotopa from 8.5 m depth (Sample 1). The second was obtained from centre of the Warsaw, namely from Jana Pawła II street, from 6 m depth (Sample 2). The soil used during the tests, which is of Quaternary origin, was sampled in an undisturbed state using a standard Shelby tube. For both samples, hydrometer tests was performed. The grain size distribution of the soil specimens are shown in Figure 3.

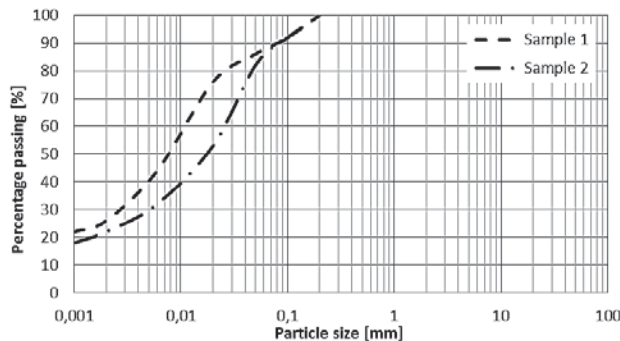


Fig. 3. Grain distribution of the tested soils

According to PN-EN ISO 14688-1:2006 the material tested by the author was silty clay (siCl). In order to compute the fundamental indices ( $w$ ,  $w_p$ ,  $w_L$ ,  $\rho$ ), standard test methods were employed. The results of the abovementioned tests are summarized in Table 1.

Table 1. The basic properties of tested soils

Parameter	Sample 1	Sample 2
	value	value
$w$ [%]	16.55	17.52
$w_p$ [%]	19.49	17.14
$w_L$ [%]	44.30	33.00
$I_p$ [%]	24.81	15.86
$I_L$ [-]	-0.12	0.02
$I_C$ [-]	1.12	0.98
$\rho$ [kg·m <sup>-3</sup> ]	2030	2140

Explanations:  $w$  is the water content;  $w_p$  is the plastic limit;  $w_L$  is the liquid limit;  $I_p$  is the plastic index;  $I_L$  is the liquidity index;  $I_C$  is the consistency index; and  $\rho$  is the mass density.

### Test equipment and research conditions

The author has performed the research using a fixed-free Stoke RC apparatus on two cylindrical specimens, about 140 mm in height and 70 mm in diameter. In this type of an RC apparatus, the bottom of the sample is permanently attached (fixed) to the lower pedestal, while the top is set in motion by the drive system located on the top cap. Torsional excitations are possible due to four magnets and four coils. In the RC triaxial chamber, a specimen is surrounded by compressed air, which – with the help of the controller – causes the required stress to occur. A detailed description of this device is contained in author's other publications [Soból et al. 2015]. The studies have been made in drained and consolidated conditions. The test was started after the saturation of the sample, when the Skempton parameter had reached the value equal to 0.95. The next step was the consolidation at the effective stress value of 85, 170, 255 and 310 kPa for the Sample 1, and 120, 180, 240, 320, 360 and 410 kPa for the Sample 2. After each stage of consolidation, resonant tests were performed at different sinusoidal wave amplitudes in order to obtain the shear strain-damping ratio growth curve and the minimal damping ratio, dependent on the mean effective stress characteristic. To find the resonant frequency of the samples, a device sets specimens in motion at a frequency varying from 5 to 200 Hz. The frequency causing the strongest shear strain to occur is designated as a resonant frequency. The investigated wave amplitudes ranged from 0.002 to 0.6 V. For each of the resonant frequencies, a damping ratio was provided. For the needs of this paper, the author has performed the calculations using both the standard HPB method (eq. 3, 4) and the modified formula (eq. 5) and subsequently compared the result with the  $D$  obtained from the FVD method.

### RESULTS

The growth curves of the FVD  $D$  depending on the shear strain at a varying effective stress level for both samples are shown in Figure 4. The above-mentioned dynamic parameter obtained by using the FVD method will be used as reference values. The shape of

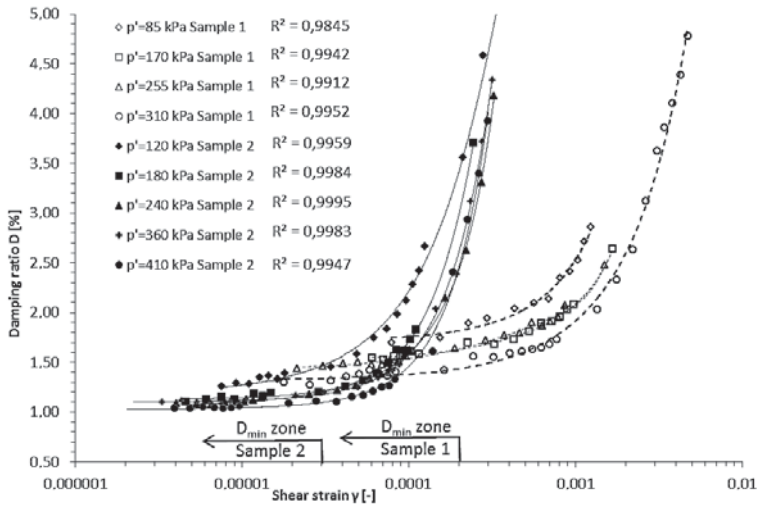


Fig. 4. FVD damping ratio  $D$  [%] depending on the shear strain  $\gamma$  [-]

each curve indicates an increase of the  $D$ , along with a simultaneous shear strain increase, present in both cases. A decrease of the  $D$ , while the effective stress level increases, can also be observed. The same phenomenon was described by the author in other publications, such as [Sas et al. 2015]. However, when the  $D$  for the Sample 2 starts to increase, the  $D$  for Sample 1 still is in own minimum values. Furthermore, the  $D_{min}$  value for Sample 1 is lower than for the Sample 2. The HPB damping ratio was calculated on the basis of resonant frequencies, using equations (3), (4) and (5). For the calculated HPB damping ratio points and damping ratio obtained from the FVD tests, a quadratic or cubic function with a very good adjustment value exceeding 0.93, has been found. On the basis of this trend, minimum damping ratio for both methods was established. In Table 2, a minimum damping for both samples at different effective stress is shown.

Table 2. Free vibration decay (FVD) minimum damping ratio  $D_{min}$  [%] and half power bandwidth (HPB) minimum damping ratio  $\zeta_{min}$  for two samples at different effective stress levels [kPa]

Effective stress [kPa]	$D_{min}$ FVD method [%]	Sample 1			Differences between $\zeta_{min}$ HPB eq. (5) and $D_{min}$ FVD method [%]	Effective stress [kPa]	Sample 2			Differences between $\zeta_{min}$ HPB eq. (5) and $D_{min}$ FVD method [%]	
		$\zeta_{min}$ HPB method [%]					$\zeta_{min}$ HPB method [%]				
		eq. (3)	eq. (4)	eq. (5)			$D_{min}$ FVD method [%]	eq. (3)	eq. (4)		eq. (5)
85	1.61	2.66	2.66	2.65	1.04	120	1.19	1.81	1.82	1.82	0.63
170	1.52	2.31	2.32	2.30	0.78	180	1.13	1.74	1.74	1.74	0.61
255	1.44	2.23	2.24	2.26	0.82	240	1.08	1.68	1.68	1.68	0.60
310	1.36	2.02	2.03	2.02	0.66	360	1.09	1.62	1.62	1.62	0.53
						410	1.03	1.55	1.55	1.55	0.52

It can be seen that the FVD method results in the damping ratio values being smaller than the HPB method. A very similar minimum damping ratio value obtained from different HPB equations can also be seen in Table 2. Despite the fact that the values of the  $\zeta_{\min}$  were comparable for all three presented HPB equations, the author has decided to compare them with the FVD damping ratio and present an entire calculated damping ratio data only for equation (5), due to its compliance with the discussed FVD dynamic parameter outside minimum damping ratio zone. In both samples differences between FVD  $D_{\min}$  and HPB  $\zeta_{\min}$  calculated from equation (5) decreases along with the effective stress increase.

The HPB damping curve dependent from the shear strain level at a varying effective stress level is presented in Figure 5. The damping ratio increases along with the increase in strain and decreases along with the increase in effective stress. Said phenomenon has appeared for both samples. The shapes of curves obtained using different research techniques are quite similar to the one obtained by using the FVD technique, which is shown in Figure 4.

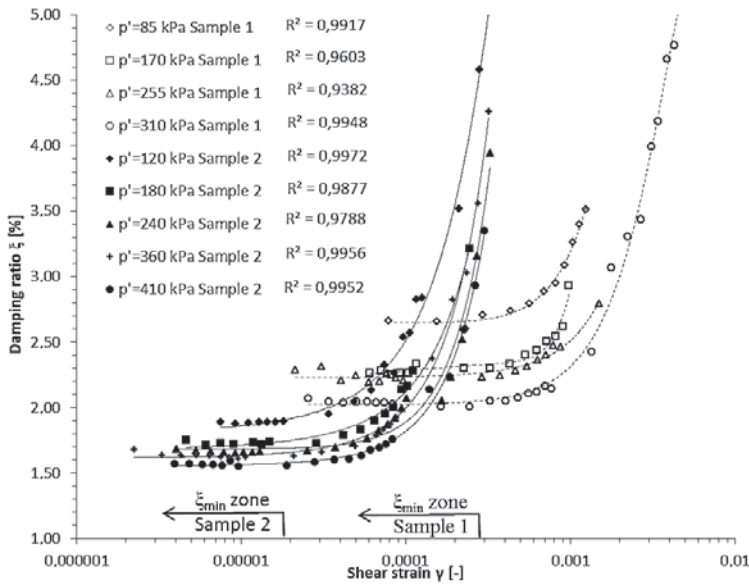


Fig. 5. HPB damping ratio  $\zeta$  [%] depending on the shear strain  $\gamma$  [-]

Despite the correct shape of the damping ratio curve obtained, by using the HPB method, the value of the discussed parameter is much bigger than the  $D$  acquired from the FVD method. The differences are the biggest in minimum damping ratio zone and decrease along with the damping ratio increase. Said phenomenon appears for both samples and is presented in Figure 6. The black line displays the FVD damping ratio, equal to the HPB damping ratio. Two dashed lines display the  $\pm 15\%$  error margin. A disagreement up to 15% in damping ratio is acceptable by ASTM [1992]. Most of the data presented in Figure 6 falls under the dashed line. This means that the HPB method overstates the



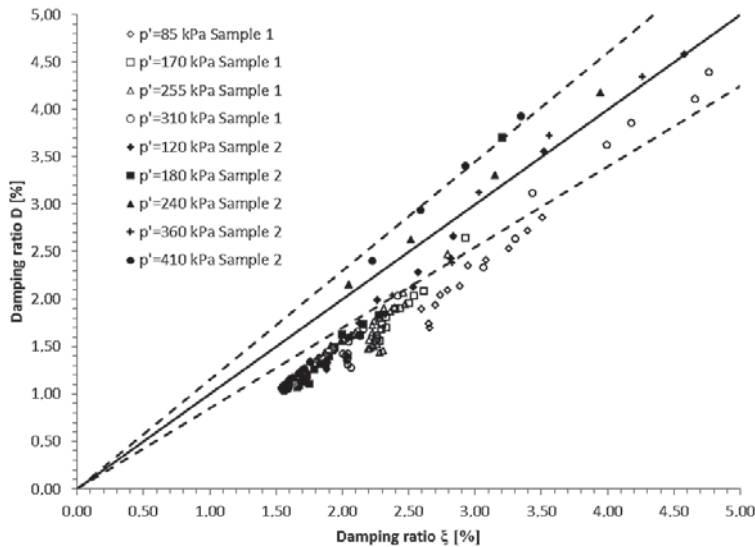


Fig. 6. FVD damping ratio  $D$  against HPB damping ratio  $\xi$

damping ratio value, especially at a low value of damping at this case from about 1% to 2.5%. Damping points bigger than 2.5% are located in the area designated by dashed lines, except for points characterised by the 85 kPa effective stress level.

## CONCLUSIONS

This article presented the results of studies conducted on the two samples of cohesive soil silty clay. Two different methods, namely the free vibration decay (FVD) and the half-power bandwidth (HPB), were adopted to examine the dynamic parameter damping ratio of said materials. The author of this paper has also used the FVD method was used for reference method. The tests were performed with the use of a resonant column apparatus. After careful analysis of obtained results, the following conclusions were reached:

1. The results of the FVD study shows that values of the  $D$  increases with the shear strain development, while the  $D_{\min}$  decreases with effective stress growth which indicates proper testing procedure.

2. Well-matched trend lines confirmed the correctness of the minimum damping ratio values for both presented methods.

3. Every used HPB equation overestimated the minimum damping ratio by 61 to 48% in case of Sample 1 and by 52 to 50% for the Sample 2.

4. In a minimum damping ratio zone, all three equations presented for the HPB method gave very similar results, but outside the mentioned zone it was equation (5) which proved to be the best fitting for the FVB method.

5. The damping ratio curve obtained from the equation (5) displayed the same trend as the FVD damping curve.

6. Despite a very significant error concerning the HPB minimum damping ratio, the author believes that the HPB method can be applied to examine damping properties of the soils, after conducting additional research and introduction correction taking into account effective stress and behaviour of the soil in minimum damping ratio zone.

7. Sample 2 reached smaller values of the minimum damping ratio, although Sample 1 was collected from at a greater depth. It is probably associated with a bigger overconsolidation stress, which occurred in case of Sample 2, however it should be confirmed by the oedometer tests.

8. It seems reasonable to compare HPB and FVD methods with another technique like steady-state vibration or damping ratio determined by torsional shear device, to finally said which technique provides correct value of the  $D_{\min}$ .

## REFERENCES

- Ahmadi, E., Khoshnoudian, F., Hosseini, M. (2015). Importance of soil material damping in seismic responses of soil-MDOF structure systems. *Soils and Foundations*, 55 (1), 35–44.
- ASTM (1992). Standard test method for modulus and damping of soils by the resonant column method: D4015-92. Annual book of ASTM standards. ASTM International, USA.
- Butterworth, J., Lee, J.H., Davidson, B. (2004). Experimental determination of modal damping from full scale testing. 13th world conference on earthquake engineering, Vancouver, Paper 310, August.
- Camacho Tauta, J.F., Santos, J.A., Viana da Fonseca, A. (2010). Strain level and vibration frequency in resonant – column tests. Proceedings of the 13th Congreso Colombiano de Geotecnia – VII Seminario Colombiano de Geotecnia, 21–24.09.2010. Manizales, Columbia (doi: 10.13140/2.1.4019.6485).
- Chopra, A.K. (1995). Dynamics of structures. Prentice Hall, New Jersey.
- Das, B., Ramana, G.V. (2010). Principles of soil dynamics. Cengage Learning, Stamford.
- Flaga, A., Szulej, J., Wielgos, P. (2008). Comparison of determination methods of vibration's damping coefficients for complex structures. *Budownictwo i Architektura*, 3, 53–61.
- Gabryś, K., Sas, W., Soból, E. (2015). Small-strain dynamic characterization of clayey soil. *Acta Sci. Pol. Architectura*, 14 (1), 55–65.
- Hoyos, L.R., Cruz, J.A., Puppala, A.J., Douglas, W.A., Suescún, E.A. (2013). Dynamic shear modulus and damping of compacted silty sand via suction-controlled resonant column testing. Proceedings of the 18th International Conference on Soil Mechanics and Geotechnical Engineering, Paris, 1125–1128.
- Ishihara, K. (1996). Soil behaviour in earthquake geotechnics. Oxford University Press, Clarendon Press.
- Lim, Y., Nguyen, T.H., Lee, S.H., Lee, J.W. (2013). Evaluation of Dynamic Properties of Trackbed Foundation Soil Using Mid-size Resonant Column Test. *International Journal of Railway*, 6 (3), 112–119.
- Magalas, L.B., Malinowski, T. (2003). Measurement techniques of the logarithmic decrement. *Solid State Phenomena*, 89, 247–260.
- Papagiannopoulos, G.A., Hatzigeorgiou, G.D. (2011). On the use of the half-power bandwidth method to estimate damping in building structures. *Soil Dynamics and Earthquake Engineering*, 31 (7), 1075–1079.
- PN-EN ISO 14688-1:2006 Badania geotechniczne. Oznaczenie i klasyfikowanie gruntów. Część 1: Oznaczenie i opis.

- Sas, W., Gabryś, K., Soból, E., Szymański, A., Głuchowski, A. (2015a). Stiffness and damping of selected cohesive soils based on dynamic laboratory tests. W: Wybrane zagadnienia konstrukcji i materiałów budowlanych oraz geotechniki. Red. M. Dobiszewska, A. Podhorecki. Wydawnictwa Uczelniane Uniwersytetu Technologiczno-Przyrodniczego, Bydgoszcz, 325–332.
- Sas, W., Gabryś, K., Szymański, A., Soból, E. (2015b). Właściwości tłumienia naturalnych gruntów spoistych w zakresie małych odkształceń. Inżynieria Morska i Geotechnika, 36 (3), 275–280.
- Senetakis, K., Anastasiadis, A., Ptilakis, K. (2015). A comparison of material damping measurements in resonant column using the steady-state and free-vibration decay methods. Soil Dynamics and Earthquake Engineering, 74, 10–13.
- Soból, E., Sas, W., Szymański, A. (2015). Zastosowanie kolumny rezonansowej do określenia reakcji gruntów drobnopziarnistych obciążonych dynamicznie. Przegląd Naukowy Inżynieria i Kształtowanie Środowiska, 68, 133–144.
- Sun, J., Gong, M., Tao, X. (2013). Dynamic shear modulus of undisturbed soil under different consolidation ratios and its effects on surface ground motion. Earthquake Engineering and Engineering Vibration, 12 (4), 561.
- Tallavo, F., Cascante, G., Sadhu, A., Pandey, M.D. (2013). New Analysis Methodology for Dynamic Soil Characterization Using Free-Decay Response in Resonant-Column Testing. Journal of Geotechnical and Geoenvironmental Engineering, 140 (1), 121–132.
- Wang, J.T., Jin, F., Zhang, C.H. (2012). Estimation error of the half-power bandwidth method in identifying damping for multi-DOF systems. Soil Dynamics and Earthquake Engineering, 39, 138–142.
- Wang, J., Lü, D., Jin, F., Zhang, C. (2013). Accuracy of the half-power bandwidth method with a third-order correction for estimating damping in multi-DOF systems. Earthquake Engineering and Engineering Vibration, 12 (1), 33–38.
- Wu, B. (2015). A correction of the half-power bandwidth method for estimating damping. Archive of Applied Mechanics, 85 (2), 315–320.
- Zhang, J., Andrus, R.D., Juang, C.H. (2005). Normalized shear modulus and material damping ratio relationships. Journal of Geotechnical and Geoenvironmental Engineering, 131 (4), 453–464.

## **PORÓWNANIE WARTOŚCI WSPÓLCZYNNIKA TŁUMIENIA GRUNTU SPOISTEGO Z LABORATORYJNYCH BADAŃ W KOLUMNIE REZONANSOWEJ UZYSKANYCH METODĄ KRZYWEJ GAŚNIĘCIA DRGAŃ SWOBODNYCH I METODĄ HALF-POWER BANDWIDTH**

**Streszczenie.** Jednym z celów we współczesnych badaniach laboratoryjnych jest poszukiwanie dynamicznych parametrów gruntu w tzw. małym zakresie odkształceń. Przyczyną takiego stanu rzeczy jest m.in. coraz gęstsza zabudowa miejska, a także ruch miejski, w tym: tramwaje, samochody, pociągi metra i niektóre rodzaje robót budowlanych, które mogą generować powstawanie małych odkształceń na styku grunt – konstrukcja. Takie odkształcenia mogą prowadzić do przekroczenia stanu granicznego używalności konstrukcji. Grunt posiada trzy główne parametry dynamiczne: moduł odkształcalności podłużnej, moduł ściskania oraz współczynnik tłumienia. Głównym celem artykułu było wyznaczenie współczynnika tłumienia gruntu spoistego metodą krzywej gaśnięcia drgań swobodnych i metodą *half-power bandwidth*. Przeprowadzono badania w kolumnie rezonansowej na dwóch próbkach iltu pylastego. Wyniki pokazują, że metoda *half-power bandwidth* przeszacowuje współczynnik tłumienia w stosunku do metody krzywej gaśnięcia drgań swobodnych od

50 do 60%. Jednak kształty uzyskanych krzywych współczynnika tłumienia w zależności od odkształcenia postaciowego są bardzo podobne. Stwierdzono, że należy przeprowadzić dalsze badania, mające na celu wprowadzenie poprawek do równań metody *half-power bandwidth*.

**Słowa kluczowe:** krzywa gaśnięcia drgań swobodnych, *half-power bandwidth*, współczynnik tłumienia, kolumna rezonansowa

Accepted for print: 21.03.2016

For citation: Sas, W. (2016). The comparison of cohesive soil damping ratios obtained from resonant column tests and designated by the free-vibration decay and half-power bandwidth method. *Acta Sci. Pol. Architectura*, 15 (1), 88–94.